

# Site-Specific Solid-State NMR Detection of Hydrogen-Deuterium Exchange Reveals Conformational Changes in a 7-Helical Transmembrane Protein

Shenlin Wang,<sup>1</sup> Lichi Shi,<sup>1,3</sup> Izuru Kawamura,<sup>2</sup> Leonid S. Brown,<sup>1</sup>  
Vladimir Ladizhansky<sup>1</sup>

<sup>1</sup>Department of Physics and Biophysical Interdepartmental Group, University of Guelph, 50 Stone Rd. E., Guelph, Ontario, Canada N1G 2W1; <sup>2</sup>Faculty of Engineering, Yokohama National University, 79-5 Tokiwadai, Hodogaya-ku, Yokohama 240-8501, Japan; <sup>3</sup>Present address: Department of Medical Genetics and Microbiology, Medical Science Building, University of Toronto, 1 King's College Circle, Toronto, Ontario, M5S1A5. Canada.

**Supporting Material**

### **Expression, purification and reconstitution of ASR**

BL21-Codonplus-RIL *E. coli* cells were transformed with a plasmid encoding C-terminally 6×His-tagged ASR truncated at position 229 (1), and cultured in M9 minimal medium at 30°C, using 4 g of uniformly labelled <sup>13</sup>C-glucose, and 1 g of <sup>15</sup>N-ammonium chloride per litre of culture as the carbon and nitrogen sources. The expression of ASR was induced by 1 mM IPTG when the cell density reached  $A_{600} = 0.4$  OD. Retinal at a concentration of 7.5 μM was added exogenously at the time of induction to regenerate the expressed opsin. The harvested cells were pre-treated with lysozyme (12 mg per litre of culture) and DNase I (600 units per litre of culture), and subsequently broken by sonication. The membrane fraction was solubilized in 1 % DDM at 4 °C, and purified following the batch procedure described in the Qiagen Ni<sup>2+</sup>-NTA resin manual. Approximately 5 mg of ASR was purified from one litre of culture. The molar amount of ASR was determined by the absorbance of opsin-bound retinal, using the extinction coefficient of 48,000 M<sup>-1</sup>cm<sup>-1</sup>.

Liposomes were prepared by hydrating dried DMPC and DMPA mixed in 9:1 ratio (w/w), and mixed with purified ASR solubilized in detergent, at a lipid:protein ratio of 1:2 (w/w). The mixture was incubated for one hour at room temperature before adding Bio-beads (Biorad) for detergent removal.

### **H/D Exchange of ASR**

Following reconstitution, ASR proteoliposomes were suspended in D<sub>2</sub>O-based NMR buffer (10 mM NaCl, 25 mM 2-(N-Cyclohexylamino)ethane sulfonic acid, pH 9) at a protein concentration of 0.4 mg/mL. The suspension was illuminated with a 100W white light source, at 22 °C (monitored throughout the experiment) under constant stirring. To prevent sample deterioration, the illumination was done in blocks of 30 minutes with 30 min interruptions until the desired illumination time was achieved. Proteoliposomes were collected by ultracentrifugation at 150,000×g for one hour for NMR experiments.

### **MAS SSNMR spectroscopy**

Approximately 11 mg of lipid reconstituted U- $^{13}\text{C}$ ,  $^{15}\text{N}$  ASR sample was transferred and center-packed in a thin wall 3.2 mm rotor. All SSNMR experiments were performed on a Bruker Avance III spectrometer operating at 800.230 MHz equipped with 3.2 mm E-free  $^1\text{H}$ - $^{13}\text{C}$ - $^{15}\text{N}$  probe (Bruker USA, Billerica, MA). The MAS frequency was 14.3 kHz and the sample temperature was maintained at 5 °C in all experiments. Three-dimensional NCACX chemical shift correlation experiments were performed using previously described pulse sequences (2,3) but without J-decoupling.

The typical  $\pi/2$  pulses were 2.5  $\mu\text{s}$  for  $^1\text{H}$ , 4  $\mu\text{s}$  for  $^{13}\text{C}$ , and 6  $\mu\text{s}$  for  $^{15}\text{N}$ .  $^1\text{H}/^{15}\text{N}$  cross-polarization (CP) (4) contact time was 300  $\mu\text{s}$ , with a constant radio-frequency (r.f.) field of 50 kHz on nitrogen, and with the proton lock field ramped linearly around  $n=1$  Hartmann-Hahn condition (5) (10% ramp, optimized experimentally).  $^{15}\text{N}/^{13}\text{C}\alpha$  transfer (6) was implemented with a contact time of 6 ms, with a constant lock field of  $2.5 \times \nu_r$  ( $\nu_r = \omega_r / 2\pi$ , spinning frequency) field strength applied on  $^{15}\text{N}$ , and with the  $^{13}\text{C}$  field ramped linearly (10% ramp) around  $1.5 \times \nu_r$ . The CW decoupling during  $^{13}\text{C}/^{15}\text{N}$  CP step was always 90 kHz. SPINAL-64 decoupling (7) of 80 kHz was used during indirect and direct chemical shift evolutions.

### **Acquisition and processing parameters**

NCACX experiments were recorded with DARR mixing time of 50 ms. Time domain data matrix was  $120(t_1) \times 172(t_2) \times 1280(t_3)$ , with  $t_1$ ,  $t_2$ ,  $t_3$  increments of 108  $\mu\text{s}$ , 41  $\mu\text{s}$ , and 16  $\mu\text{s}$ , respectively. The carrier frequency was placed at 118 ppm and 55 ppm for nitrogen and carbon chemical shift evolution, respectively. 8 scans per point were recorded, with a recycle delay of 1.8 s. Data were processed with Lorentzian-to-Gaussian apodization functions and zero filled to  $1024(t_1) \times 1024(t_2) \times 4096(t_3)$  prior to Fourier Transform. 16 Hz of Lorentzian line narrowing and 40 Hz of Gaussian line broadening were applied in the  $t_1$   $^{15}\text{N}$  indirect dimension, 40 Hz of Lorentzian line narrowing and 80 Hz of Gaussian line broadening were applied in the  $t_2$   $^{13}\text{C}\alpha$  indirect and the  $t_3$   $^{13}\text{C}\alpha$  direct dimensions, respectively.

### **H/D exchange data analysis**

The carbon chemical shifts were indirectly referenced to 2,2-dimethyl-2-silapentane-5-sulfonic acid (DSS) by adjusting the position of the  $^{13}\text{C}$  adamantane downfield peak to 40.48 ppm (8). The nitrogen chemical shifts were referenced indirectly (9) by using the ratio of gyromagnetic ratios  $\gamma_{\text{N}}/\gamma_{\text{C}}=0.402979946$ , taken without a temperature factor correction (10). Experimental data were processed with NMRPipe (11). Peak picking and noise analysis were performed with the CARA software (12).

Noise statistics was analyzed for a signal-free 3D box containing  $\sim 10^6$  points in each of the 3D spectra by running a suite of in-house-built LUA scripts in the CARA environment. A cutoff of  $5\sigma$  was chosen for peak picking. Only isolated cross peaks were considered in the analysis.

For each amino acid, the intensities of all resolved N-CA-CX (i.e., N-CA-CA, N-CA-CB, N-CA-CO, etc.) cross peaks were added for each of the experiments. Some amino acids are fully resolved even in the 2D NCA spectrum (Fig. S2), while many others require 3D spectroscopy for a complete resolution. Consequently, well resolved residues, and in particular those with well resolved NCA peaks (Fig. S2) will have higher peak intensity (sum of N-CA-CA, N-CA-CB, peaks, etc.). This explains great variability of the intensities in Fig. 1. For presentation purposes in Figs. S1 and 2 all residues were conservatively classified into two groups of exchangeable (cross peak intensities in  $\text{D}_2\text{O}$ -incubated samples are attenuated by at least a factor of four compared to the fully protonated sample) and non-exchangeable. The latter include some residues with cross-peak intensities attenuated in  $\text{D}_2\text{O}$ , but not to the extent observed for the completely exchangeable residues.

To correct spectral intensities for slight variation of sample amount in the rotor, we collected  $^{13}\text{C}$  CP spectra (CP mixing time of 2 ms), and used the intensities of the aliphatic side chains, primarily  $\text{CH}_3$  groups, for normalization. These carbons are far away from the backbone nitrogens, and draw their polarization primarily from their directly attached protons. Their signals are independent of the amide protonation states and can therefore be used for normalization.

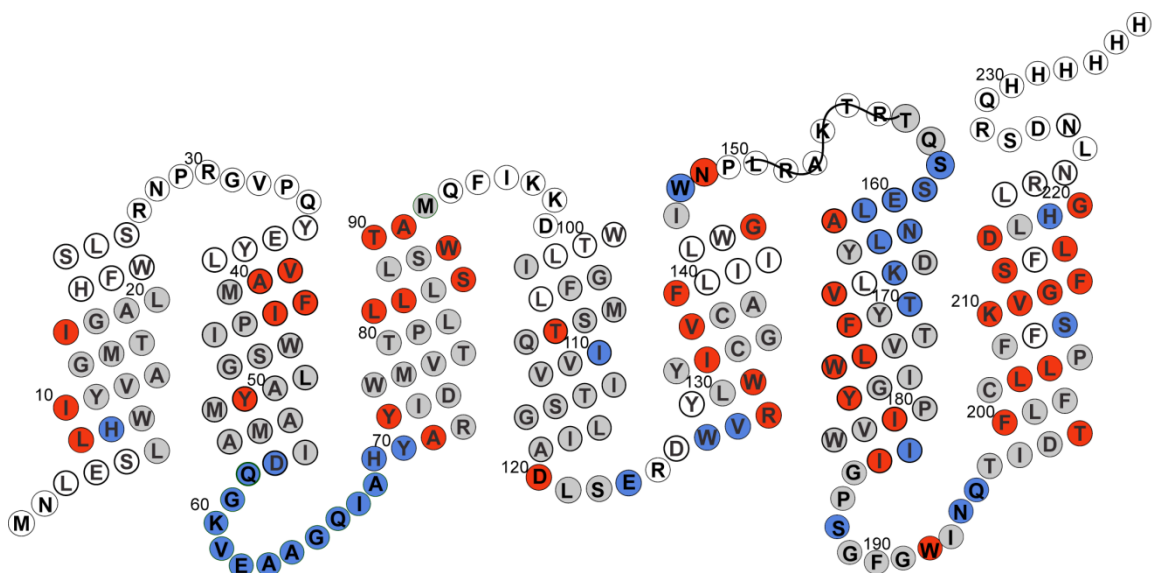


**Figure S1.** Amino acid sequence and colour representation of residues affected by H/D exchange. Blue are exchangeable in the dark, red are exchangeable under illumination (4.5 h), grey are non-exchangeable (note that those include residues with moderate decrease in the cross-peak intensities), and white are unassigned residues.

Thus, we conclude that cross peaks in the 2D and 3D NCACX (Fig. S3) spectra can be used to qualitatively assess the extent of the H/D exchange of amide protons. We do note, however, that the suppression of NCA correlations may be incomplete, with as much as  $\sim 25\%$  of the signal remaining. Although even better excitation selectivity can, in principle, be achieved by further shortening the CP time, this results in overall sensitivity losses, and was not used in this study.

### Error estimation

Spectrometer performance is stable over prolonged periods of time (many months) as confirmed by the consistency of data collected on multiple samples, including standards, like glycine and microcrystalline sample of GB3, and proteorhodopsin and ASR. Signal intensities in Figure 1 (main manuscript) are given in the units of root mean square (RMS) of noise and provide direct measure of random error. It is generally much more difficult to estimate systematic errors. Among them are (i) residual CP signal, which is expected even in fully back-exchanged residues. We estimate from proline signals that this contribution should not exceed 25% of the signal from protonated

residues, and typically is much less. (ii) Inaccurate extractions of peak intensities, which are in turn related to spectral overlap, imperfect phasing, etc. All these sources cumulatively contribute to a slight variation of peak intensities of non-exchangeable residues between experiments with different illumination times. There are a few instances, when the intensity unexpectedly increases after additional 3 h of illumination. For the majority of cases these increases are within  $3\sigma$ . Notable exceptions are residues 46, 50, 103, 120, 139, and 199, for which the increase is in the range of  $5\sigma$ - $9\sigma$ . However, with the exception of Ala50, these peaks are very weak and below the cutoff of  $5\sigma$  in the 1.5 h spectrum, and are only slightly above the cutoff in the 4.5 h spectrum. Ala50 has about 20% higher intensity in the 4.5 h spectrum, which gives a rough estimate of the systematic errors.

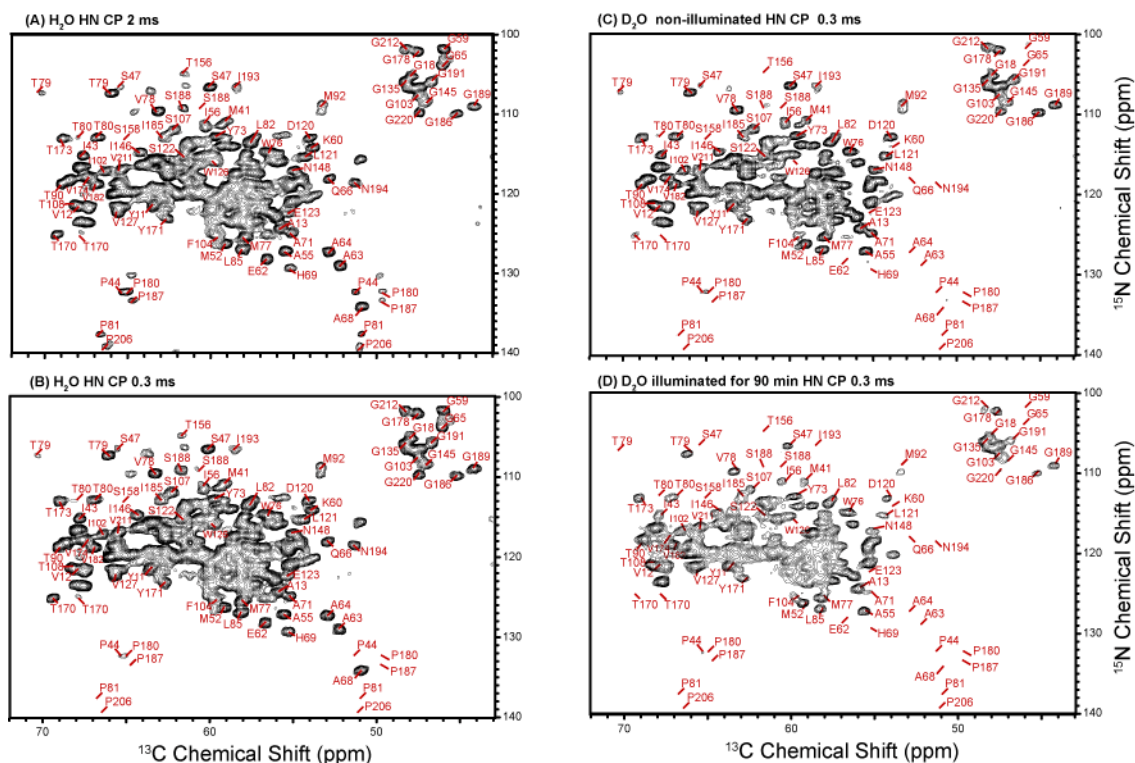


**Figure S2.** A comparison of 2D NCA spectra of ASR incubated under different conditions and collected with different CP times as indicated in the figures.

### Effects of CP mixing time and H/D exchange on the intensity of cross peaks in $^{15}\text{N}$ - $^{13}\text{C}$ correlation spectra

ASR gives 2D NCA spectra of high resolution as shown in Fig. S2A, where many individual cross peaks are fully resolved. A noteworthy feature of this spectrum is the

presence of a large number of proline correlations, both of NCA and NCD type, which are driven by “long-range”  $^1\text{H}/^{15}\text{N}$  (e.g., at least two-bond) polarization transfer processes. On average, their cumulative intensities are roughly two thirds of the correlations of non-prolyl NCA signals. Shortening the CP time to 300  $\mu\text{sec}$  (Fig. S2B) results in general attenuation of the non-prolyl cross peaks ( $\sim 70\text{-}75\%$  of the original intensity is retained), and in disappearance of most of proline peaks, indicating that under these conditions, the long-range transfer is significantly attenuated. The only noticeable exception is at the position of two overlapping NCA correlations of P44 and P180, which about four times weaker than in the spectrum with 2 ms HN CP mixing.

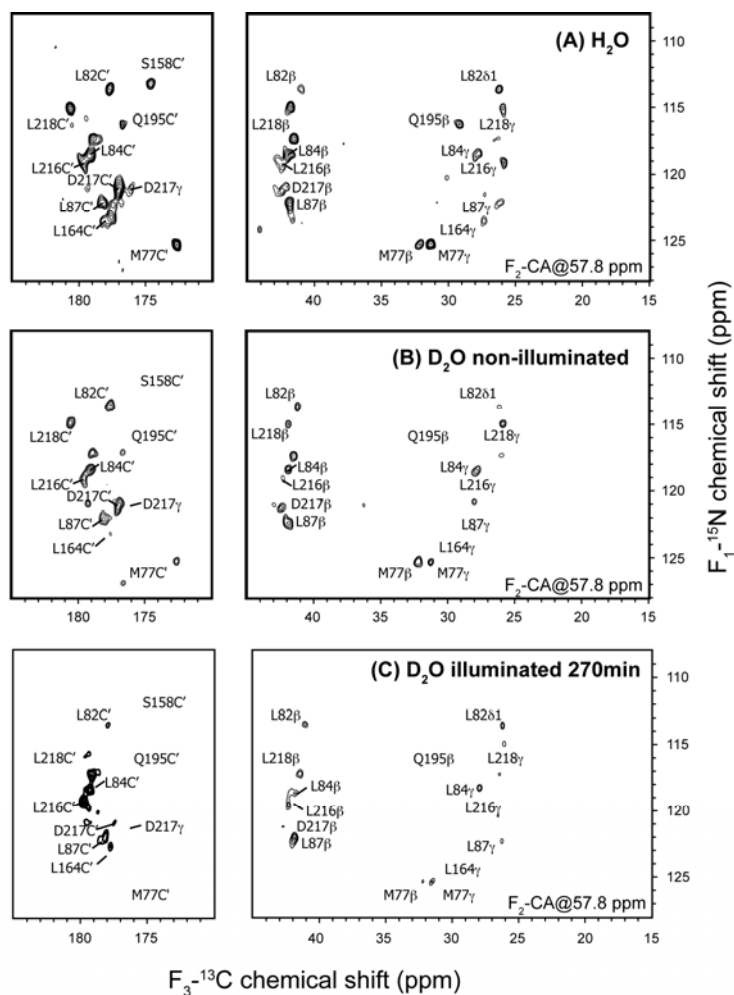


**Figure S3.** A comparison of selected 2D NC planes from the 3D NCACX correlation spectra collected in samples incubated in (A)  $\text{H}_2\text{O}$ , (B)  $\text{D}_2\text{O}$  in the dark, and (C)  $\text{D}_2\text{O}$  illuminated for 270 min. Reduction of cross peak intensities in (B) and (C) indicates an increasing level of deuteration upon illumination.

Incubation in D<sub>2</sub>O in the dark results in disappearance and attenuation of many cross peaks in the spectra (Fig. S2C), as discussed in the main text. Further attenuation can be seen when exchange is performed under illumination (Fig. S2D, S3).

## REFERENCES

1. Shi, L. C., S. R. Yoon, A. G. Bezerra, K. H. Jung, and L. S. Brown. 2006. Cytoplasmic shuttling of protons in Anabaena sensory rhodopsin: Implications for signaling mechanism. *J Mol Biol* 358:686-700.
2. Shi, L., X. Peng, M. A. Ahmed, D. A. Edwards, L. S. Brown, and V. Ladizhansky. 2008. Resolution enhancement by homonuclear J-decoupling: application to three-dimensional solid-state magic angle spinning NMR spectroscopy. *J Biomol Nmr* 41:9-15.
3. Shi, L., M. A. M. Ahmed, W. Zhang, G. Whited, L. S. Brown, and V. Ladizhansky. 2009. Three-Dimensional Solid-State NMR Study of a Seven-Helical Integral Membrane Proton Pump—Structural Insights. *J Mol Biol* 386:1078-1093.
4. Pines, A., M. G. Gibby, and J. S. Waugh. 1973. Proton-Enhanced NMR of Dilute Spins in Solids. *J Chem Phys* 59:569-590.
5. Hartmann, S. R. and E. L. Hahn. 1962. Nuclear Double Resonance in the Rotating Frame *Physical Review* 128:2042-2053.
6. Baldus, M., A. T. Petkova, J. Herzfeld, and R. G. Griffin. 1998. Cross polarization in the tilted frame: assignment and spectral simplification in heteronuclear spin systems. *Mol Phys* 95:1197-1207.
7. Fung, B. M., A. K. Khitrin, and K. Ermolaev. 2000. An improved broadband decoupling sequence for liquid crystals and solids. *J Magn Reson* 142:97-101.
8. Morcombe, C. R. and K. W. Zilm. 2003. Chemical shift referencing in MAS solid state NMR. *J Magn Reson* 162:479-486.
9. Cavanagh, J., W. J. Fairbrother, A. G. Palmer, and N. J. Skelton. 1996. *Protein NMR Spectroscopy: principles and practice*. San Diego: Academic Press. 587 p.
10. Markley, J. L., A. Bax, Y. Arata, C. W. Hilbers, R. Kaptein, B. D. Sykes, P. E. Wright, and K. Wuthrich. 1998. Recommendations for the presentation of NMR structures of proteins and nucleic acids - IUPAC-IUBMB-IUPAB inter-union task group on the standardization of data bases of protein and nucleic acid structures determined by NMR spectroscopy. *Eur J Biochem* 256:1-15.
11. Delaglio, F., S. Grzesiek, G. W. Vuister, G. Zhu, J. Pfeifer, and A. Bax. 1995. Nmrpipe - a Multidimensional Spectral Processing System Based on Unix Pipes. *J Biomol Nmr* 6:277-293.
12. Keller, R. 2004. *The Computer Aided Resonance Assignment Tutorial* Goldau CANTINA Verlag